DOI: 10.4408/IJEGE.2016-02.O-05

DETECTION OF NANOSEISMIC EVENTS RELATED TO SLOPE INSTABILITIES IN THE QUARRY DISTRICT OF CORENO AUSONIO (ITALY)

Matteo FIORUCCI(*), Roberto IANNUCCI(*), Salvatore MARTINO(*) & Antonella PACIELLO(**)

(*)Sapienza Università di Roma - Dipartimento di Scienze della Terra e Centro di Ricerca CERI - Piazzale Aldo Moro, 5 - 00185 Roma, Italy
(**)ENEA - C.R. Casaccia - Via Anguillarese, 301 - 00123 Roma, Italy
Corresponding author: roberto.iannucci@uniroma1.it

EXTENDED ABSTRACT

Le cave per l'estrazione di materiale roccioso rappresentano contesti in cui possono aver luogo eventi di instabilità gravitativa causati dalle continue sollecitazioni cui sono soggette le pareti produttive, principalmente connesse alle vibrazioni dovute alle esplosioni necessarie alle operazioni di disgaggio. La necessità di gestione del rischio da frana per la salvaguardia del personale impegnato nell'attività estrattiva ha portato, nel tempo, alla richiesta di attivare sistemi di monitoraggio nelle aree di coltivazione mineraria e di cava.

Nel presente lavoro il monitoraggio nanosismometrico, una tecnica di geofisica passiva recentemente sviluppata per le indagini di microsismicità, è stato impiegato nel distretto di cave a cielo aperto di Coreno Ausonio (in provincia di Frosinone). Il monitoraggio nanosismometrico consente l'individuazione e la localizzazione di deboli eventi sismici, fino a magnitudo locale (M_L) nell'ordine di -3, attraverso l'impiego di quattro sensori sismometrici disposti secondo una specifica geometria di *array* detta SNS (*Seismic Navigation System*).

Dopo aver individuato una cava in cui erano programmate esplosioni per la volata delle pareti in roccia, nel corso del 2013 sono state organizzate 3 campagne di acquisizione durante tre giornate, pianificate in modo da monitorare l'area in un periodo compreso da qualche ora prima dell'esplosione alle 24 ore successive. Su una parete della cava non più produttiva è stato effettuato un rilevamento geologico-tecnico che ha permesso di individuare 4 principali sistemi di discontinuità e caratterizzarli in termini di giacitura, resistenza, rugosità, apertura, spaziatura e condizioni idrauliche secondo gli standard ISRM (1978). L'analisi di stabilità della parete in esame, tenuto conto della sua orientazione, ha restituito una scarsa propensione ad eventi di instabilità.

Analizzando mediante il *software* NanoseismicSuite i dati sismometrici acquisiti è stato possibile ottenere i "supersonogrammi", ovvero particolari spettrogrammi auto-adattanti alle variazioni del rumore sismico di fondo, dai quali sono state definite alcune caratteristiche specifiche di forma d'onda per diverse tipologie di eventi. In base ai supersonogrammi, è stato possibile individuare e localizzare 15 esplosioni, di cui 3 provenienti dalla cava di riferimento e 12 da cave adiacenti del distretto, e 27 deboli eventi di instabilità gravitativa, distinti in 23 eventi di collasso e 4 rotture legate alle fratturazione dell'ammasso roccioso. Le 3 esplosioni avvenute nella cava di riferimento, e quindi aventi coordinate di origine nota, sono state utilizzate per calibrare il modello di sottosuolo, successivamente impiegato per localizzare gli altri eventi registrati.

Le rotture sono risultate originate in diverse zone del distretto estrattivo, mentre gli eventi di collasso sono stati localizzati in una specifica area e risultano essere avvenuti prevalentemente in un limitato intervallo di tempo a seguito delle 9 esplosioni registrate nella campagna del 26-27 luglio 2013. Non è stato possibile, invece, individuare eventi riconducibili ad instabilità negli orari di attività di cava a causa dell'elevato livello di rumore apportato dagli strumenti per l'estrazione e la lavorazione del materiale roccioso. Si è escluso che gli eventi di collasso fossero riconducibili direttamente all'attività di estrazione sia perché registrati al di fuori dell'orario di lavorazione delle cave sia perché, analizzando l'intera registrazione per intervalli orari, le frequenze tipiche dei macchinari di lavorazione non sono risultate energizzante. La zona di origine è risultata essere un'area nella quale sono stati rinvenuti detrito sciolto costituito da blocchi eterometrici ed una parete non in coltivazione con medesime caratteristiche delle discontinuità rispetto alla parete sulla quale era stato effettuato il rilevamento geologico-tecnico, ma con diversa orientazione.

In definitiva, la fase di sperimentazione ha restituito dei risultati di indubbio interesse consentendo di mettere in evidenza alcune limitazioni del monitoraggio nanosismometrico nel contesto preso in esame, in particolare legate all'eccessiva rumorosità registrata nelle ore di attività di cava. La tecnica appare, comunque, un utile strumento di monitoraggio per i fenomeni gravitativi di debole intensità, in grado di contribuire alla gestione del rischio da frana in aree ad elevata attività antropica ed in ambienti naturalmente predisposti ad instabilità gravitative che possono interessare pareti in roccia.

ABSTRACT

Nanoseismic monitoring is a passive geophysical technique used to identify and locate weak seismic events (down to local magnitudes, M_L, around -3). This technique was applied in the open-pit quarry district of Coreno Ausonio (central Italy) to detect possible gravity-induced slope instabilities resulting from quarry rock blasting. After identifying an active quarry, an engineering-geological survey was carried out to characterise the jointed rock mass on an abandoned wall in front of the quarry. Four main joint sets were surveyed and their geometric and mechanical properties were measured in order to carry out stability analyses that evidenced scarce proneness to failure of the investigated wall. The analysis of seismic records obtained during three monitoring surveys, performed through the NanoseismicSuite software, made it possible to detect and characterise 15 blasts, of which 3 from the reference quarry and 12 from nearby quarries within the district, as well as 27 weak slope instability events (23 collapses and 4 failures). While failures originated from different areas of the quarry district, collapses occurred in a site characterised by an abandoned quarry having a wall more prone to gravity-induced instabilities than the one previously characterised.

Keywords: *nanoseismic monitoring, landslide risk, failure, collapse, quarry activity*

INTRODUCTION

Protection of the personnel involved in quarrying against the landslide risk has led over time to a demand for monitoring quarry sites. The removal of rock from these sites may induce gravitational instabilities due to sudden changes of the quarry wall shape and/or to vibrations associated with blasting, as demonstrated by controlled blasting tests in quarry sites (Phillips *et alii*, 1997).

Indeed, changes in the stress-strain state of a jointed rock mass may trigger fast and violent landslides affecting entire slopes (Evans *et alii*, 2006). The study of rock mass microseismicity, in terms of space-time event sequences, may contribute to mitigate the landslide risk, as well as to design and put in place monitoring systems for early warning. In the past decade, based on observations of microseismic sequences as precursors of major rock mass ruptures (Szwedzicki, 2003), considerable progress was made in the study of seismic precursors of landslides via monitoring networks, equipped with geophones or seismic sensors (Deparis *et alii*, 2008; Amitrano *et alii*, 2010; Got *et alii*, 2010; Lenti *et alii*, 2012). Monitoring systems capable of recording and characterising space-time sequences of seismic events initiating landslides are not only useful tools for tracking landslides and ultimately ensure the safety of people and property in real time, but they have also shed more light on gravity-induced instabilities. For instance, the study of data collected by high-resolution seismic monitoring systems installed in the deep mines of Canada and Australia (Hudyma & Potvin, 2010) or in hydroelectric power plants in China (Tang *et alii*, 2015) has helped define specific rock mass volumes where microseismic events originate. These volumes are those where deformations take place because of predisposing geological features and/or changes in their stress-strain state. Within these rock mass volumes, one or more microseismic sources were spotted and characterised.

This paper focuses on the findings from an experiment of nanoseismic monitoring (Joswig, 2008), a passive geophysical technique that enables to identify and localise weak seismic events down to magnitude M_L around -3, in the quarry district of Coreno Ausonio (central Italy). The experiment was expected to test nanoseismic monitoring in a setting where fast morphological changes due to continuous quarrying and associated vibrations (especially those induced by blasting) might give rise to gravity-induced slope instabilities.

TEST SITE

GEOLOGICAL SETTING

The quarry district of Coreno Ausonio (central Italy) is part of the geological complex of the Lepini-Ausoni-Aurunci Mountains. The stratigraphic succession of the area consists of a powerful sedimentary body of Meso-Cenozoic age belonging to the Latium-Abruzzi series (Accordi *et alii*, 1986), which was stacked and overthrust in the Miocene and, finally, partially covered by present and Plio-Pleistocene sediments in morphological depressions (Bally *et alii*, 1988; Cipollari & Cosentino, 1997). The Ausente river valley and part of the Latina valley were emplaced along the thrust fault lines through which the limestones of the western Aurunci Mountains were thrust over the Miocene flysch.

The quarry district lies on the eastern slope of the Ausente river valley (Fig. 1), where the neritic stratigraphic series of the Ausoni-Aurunci Mountains is exposed (Accordi *et alii*, 1969; Cipollari & Cosentino, 1992). Above the basal dolomites (Norian) lies a powerful succession of Cretaceous-Jurassic age, also known as the series of the Mesozoic carbonates of the eastern Aurunci (Putignano & Ungaro, 1996). The succession includes alternating micritic limestones, detrital limestones, calcarenites and dolomites. The most recent formation is the *Calcari bianchi e avana* (Cenomanian-Danian), that overlaps the *Calcari a briozoi e litotamni* (Langhian-Serravallian), the *Marne ad Orbulina* (Serravallian-Tortonian) and the *Flysch argilloso-arenaceo* (Tortonian-Messinian). The *Calcari a briozoi e litotamni* - bioclastic limestones interbedded with detrital-organogenic limestones and fine calcarenites – outcrop all along the eastern slope of the Ausente river valley, which comprises the area under review. It is on this outcrop that the modern "Perlato Royal Coreno" marble quarries were opened in the mid-20th century. These quarries hosted the experimental activities discussed here.

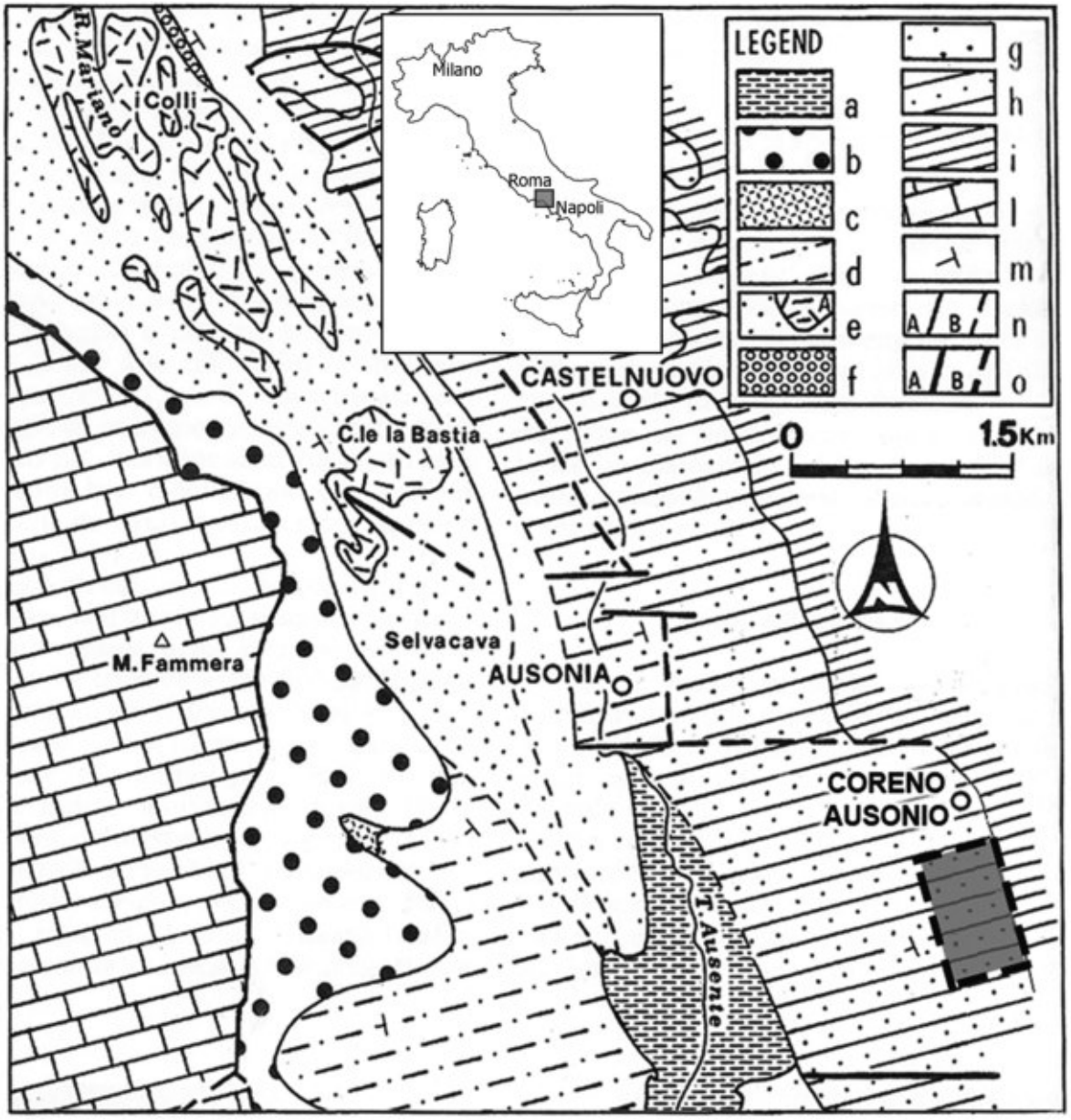

Fig. 1 - a) Geological sketch of the Ausente river valley. LEGEND: a) recent alluvial deposit (Quaternary); b) slope breccia (Quaternary); Flysch argilloso-arenaceo: c) Piscimola unit (upper Messinian), d) Fornaci Pontine unit (lower Messinian), e) Monte Bracchi unit (lower Messinian), f) Arenella unit (Tortonian-Messinian), g) Pietraroia formation (middle-upper Tortonian); h) Marne ad Orbulina (Serravallian-Tortonian) and Calcari a briozoi e litotamni (Langhian-Serravallian); i) Mesozoic carbonates of the eastern Aurunci mountains; l) Mesozoic carbonates of the western Aurunci mountains.; m) attitude of beds; n) stratigraphic contacts, exposed (A) and assumed (B); fault contacts, exposed (A) and assumed (B); the grey rectangle shows the quarry district of Coreno Ausonio (modified after Putignano & Ungaro, 1996)

The morphological evolution of the eastern slope of the Ausente river valley created a fairly gentle upward slope, marked by abrupt slope ruptures associated with the occurrence of quarries and karst landforms (Brunamonte *et alii*, 1996). Quarrying activities have strongly modified the shape of the slope which hosts the Coreno Ausonio quarry so that the dominant and typical landforms are presently represented by benches (see the profile in Fig. 9). Quarrying by blasting and removal of rock volumes caused a rapid evolution of the slope, which generated local gravity-induced instabilities of more or less small rock volumes from the sub-vertical quarried walls.

ROCK MASS GEOMECHANICAL CHARACTERISATION

An in-situ engineering-geological survey was carried out to define the mechanical properties of the rock mass in terms of attitude (i.e. dip direction and dip), strength and stiffness of the joints. This survey was performed on a rock wall that was regarded as typical of the joint sets existing in the quarry district. This rock wall, no longer quarried (hereafter called "reference wall"), is located in front of the quarry (hereafter called "reference quarry") where the blasts have been executed during 2013 (Fig. 2).

The engineering-geological survey pointed out four joint sets on the investigated wall (Fig. 3): S1 identifies the bedding of the *Calcari a briozoi e litotamni* outcrop, whereas S2, S3 and S4 indicate the sets of joints of non-sedimentary origin. According to the ISRM (1978) standard, each of the identified joint systems was characterised by defining its attitude (Fig. 4), JCS (Joint Compression Strength) coefficient (indicating the joint wall compressive strength, determined through sclerometer tests by the Schmidt hammer), JRC (Joint Roughness Coefficient) coefficient (indicating the joint wall roughness, determined via a profilometer), aperture, joint spacing, filling and hydraulic flow. The maximum friction angle, ϕ, was derived from the above values through the following relation proposed by Barton & Choubey (1977):

$$\phi = [JRC \log_{10} (JCS/\sigma_n) + \phi_r]$$

where σ_n is the effective normal stress computed at the half of the reference wall and ϕ_r is the residual friction angle derived through the relation:

Fig. 2 - Satellite view showing the SNS array installed in the quarry district of Coreno Ausonio: the "reference wall" is shown by the green ellipse, the "reference quarry" by the blue ellipse and the blasts of known location by the red stars

$$\phi_r = (\phi_b\text{-}20°) + 20\ (r/R)$$

in which ϕ_b is the basic friction angle, r is the Schmidt hammer rebound value on weathered joint surface and R is the Schmidt hammer rebound value on unweathered rock surface.

For the matrix of the jointed rock mass, the uniaxial compressive strength, σ_c, measured with the point load test (ASTM, 2008), resulted to be 152.8 MPa. Table 1 summarises the geomechanical properties of the four joint sets identified in the jointed rock mass.

The stability of the reference wall, i.e. its proneness to failures

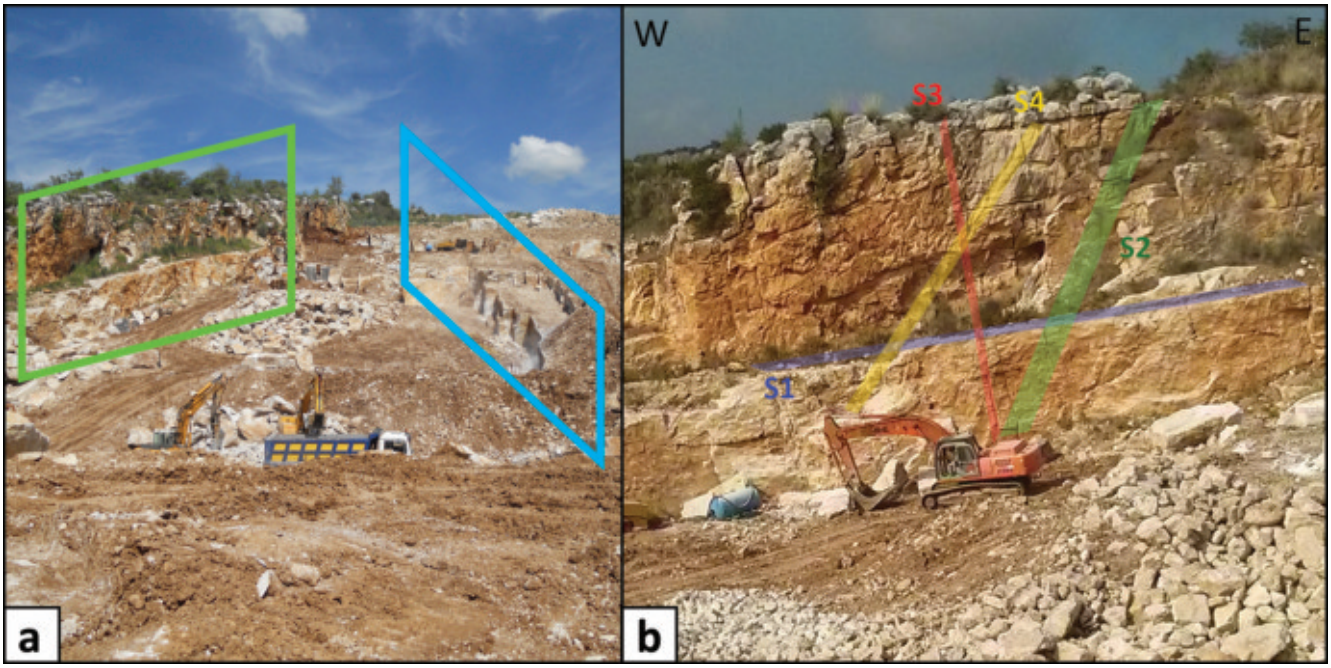

Fig. 3 - Test site: a) photo of reference wall (green parallelogram) and reference quarry with rock excavation by blasting (blue parallelogram); b) photo (W-E orientation) of the reference wall highlighting the four identified joint sets (S1, S2, S3, S4)

according to typical mechanisms of rock slopes (wedge sliding, planar sliding and toppling), was evaluated by Markland (1972) tests. As it regards planar sliding and toppling, the attitude of the identified joint sets failed to satisfy the kinematic constraints required for failure (Hoek & Bray, 1981). Consequently, the occurrence of instability events of this type was ruled out. Moreover, wedge sliding was analysed via the open-source Wedge Failure Analysis software, developed by the Southern Illinois University (SIU). Under the criteria proposed by Hoek & Bray (1981), this software carries out two tests on pairs of planar systems: i) the kinematic compatibility test (Markland, 1972), based on the attitude of the investigated elements; and ii) the dynamic compatibility test, using the geomechanical parameters of the rock mass to determine a safety factor (SF) for wedge sliding computed under global limit equilibrium (GLE) assumptions. The results from the GLE analyses yielded SF values of almost 2 for wedge sliding, suggesting a low suitability for this gravity-induced instability mechanism.

Nevertheless, also external stresses should be considered. For instance, daily and repeated blasting and working in the quarry district may negatively affect quarry wall stability and potentially trigger landslides.

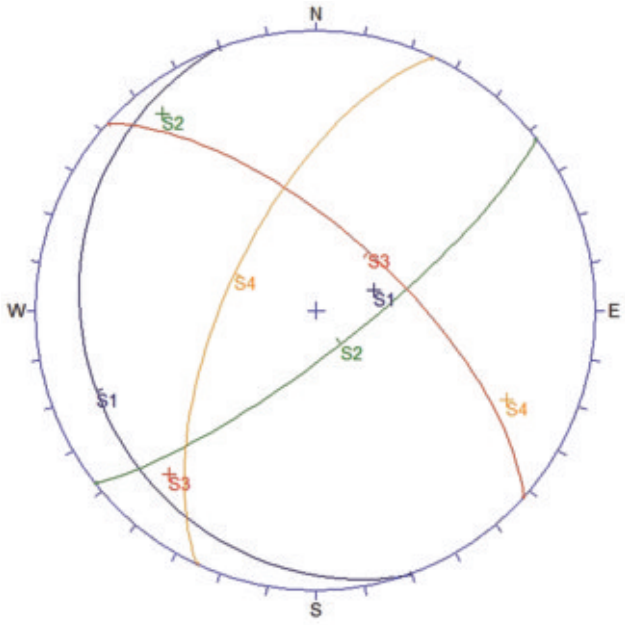

Fig. 4 - Stereographic plot (equiareal from the lower Schmidt hemisphere) of the four identified joint sets (S1, S2, S3, S4)

ACQUISITION AND PROCESSING OF SEISMIC DATA

Nanoseismic monitoring (Joswig, 2008) has been recently proposed for microseismic investigations and has filled the gap between microseismic networks and passive seismic, permitting to record as well as characterise seismic events down to M_L -3.0. The seismic data recorded by a specific-geometry array, called Seismic Navigation System (SNS), can be managed by the NanoseismicSuite software (www.nanoseismic.net), developed by the Institute of Geophysics of the Stuttgart University, which includes two main tools: SonoView and HypoLine. SonoView screens the data via the supersonogram operator, i.e. a specific spectrogram with noise adaptation, muting and pre-whitening function and a special colour palette that facilitates visual detection of seismic events (Sick *et alii*, 2014). The main advantage of sonograms is that they highlight event-related signals from stationary background noise (Joswig, 1995), using the "memory image" concept as a detection tool (Joswig, 1990). Stationary noise unrelated to the signal is filtered, allowing for a reliable detection even under challenging noise conditions. Moreover, events are localised with HypoLine (Joswig, 2008): this tool, based on a seismological approach, designs several shapes (i.e. 4 circles, 6 hyperboles, 2 beams) for locating the event source after a manual first-arrival picking of the signal time-histories. This permits to assess the hypocentre location as well as the M_L of the detected microseismic events. Several experiments (Wust-Block & Joswig, 2006; Walter *et alii*, 2012a, 2012b; Sick *et alii*, 2014; Fiorucci *et alii*, 2016) demonstrated the reliability of nanoseismic monitoring to detect and locate vibrational events related to rock mass instabilities, e.g. landslides and sinkholes.

Joint set	Dip direction and dip (°)	JCS (MPa)	JRC	Aperture (cm)	Spacing (m)	Filling	Hydraulic conditions	ϕ_r (°)	ϕ (°)
S1	250/18	122.4	8-10	-	2	-	No flow	26.9	56.3
S2	142/78	202.3	14-16	0-2	1.5	None	No flow	28.3	80.6
S3	42/67	131.8	8-10	0-0.2	1.5-2	Clayey soil	No flow	27.1	56.8
S4	295/64	166.3	14-16	0-0.5	2.5	Red soils and concretions	No flow	27.7	78.8

Tab. 1 - Summary of the geomechanical properties attributed to the joint sets surveyed on the quarry wall

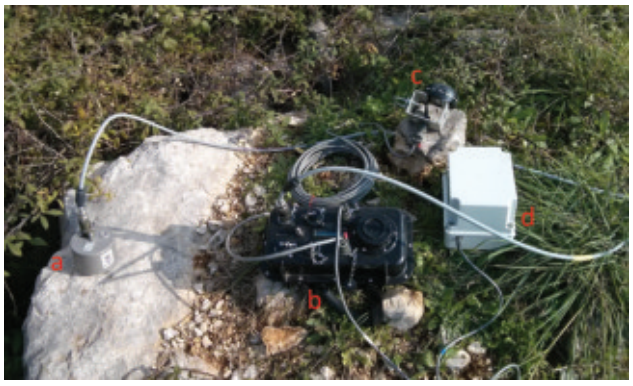

Fig. 5 - Single SNS array station: Lennartz Electronic GmbH LE-3Dlite MkII seismometer (a), REFTEK 130-01 data recorder (b) with GPS antenna (c) and battery (d)

A SNS array, consisting of a three-component seismometer and three vertical seismometers, spaced 40-50 m apart from each other (Fig. 5), was installed about 300 m away from the reference quarry during the three surveys carried out in the following periods: i) 31 May-1 June, ii) 26-27 July, iii) 29-30 October 2013. Each station was equipped with an LE-3Dlite MkII seismometer (Lennartz Electronic GmbH) and a REFTEK 130-01 acquisition unit, which was set up to record data continuously at a sampling frequency of 500 Hz. Each survey was planned according to the blasting schedule in the reference quarry, to record data over a period going from a few hours before the blast to the 24 following hours.

The data collected during the three measurement campaigns were analysed with the NanoseismicSuite SonoView tool, thus identifying 15 blasts, of which 3 from the reference quarry and 12 from nearby quarries within the district, as well as 27 events related to gravity-induced slope instability. Among the latter events, 23 collapses and 4 failures were distinguished based on signal duration and frequency content (Fiorucci *et alii*, 2016). Using the HypoLine tool to the identified events it was possible to define their epicentre, hypocentre and M_L. The accuracy of the hypocentre accounted for about 10% of the array-source distance, implying a ±0.1 uncertainty on the value of M_L (Walter *et alii,* 2012b). Finally, specific scripts running in Unix environment and using the SAC (Seismic Analysis Code) software enabled to physically characterise the recorded events and to compute PGA (Peak Ground Acceleration), PGV (Peak Ground Velocity) and AI (Arias Intensity) values.

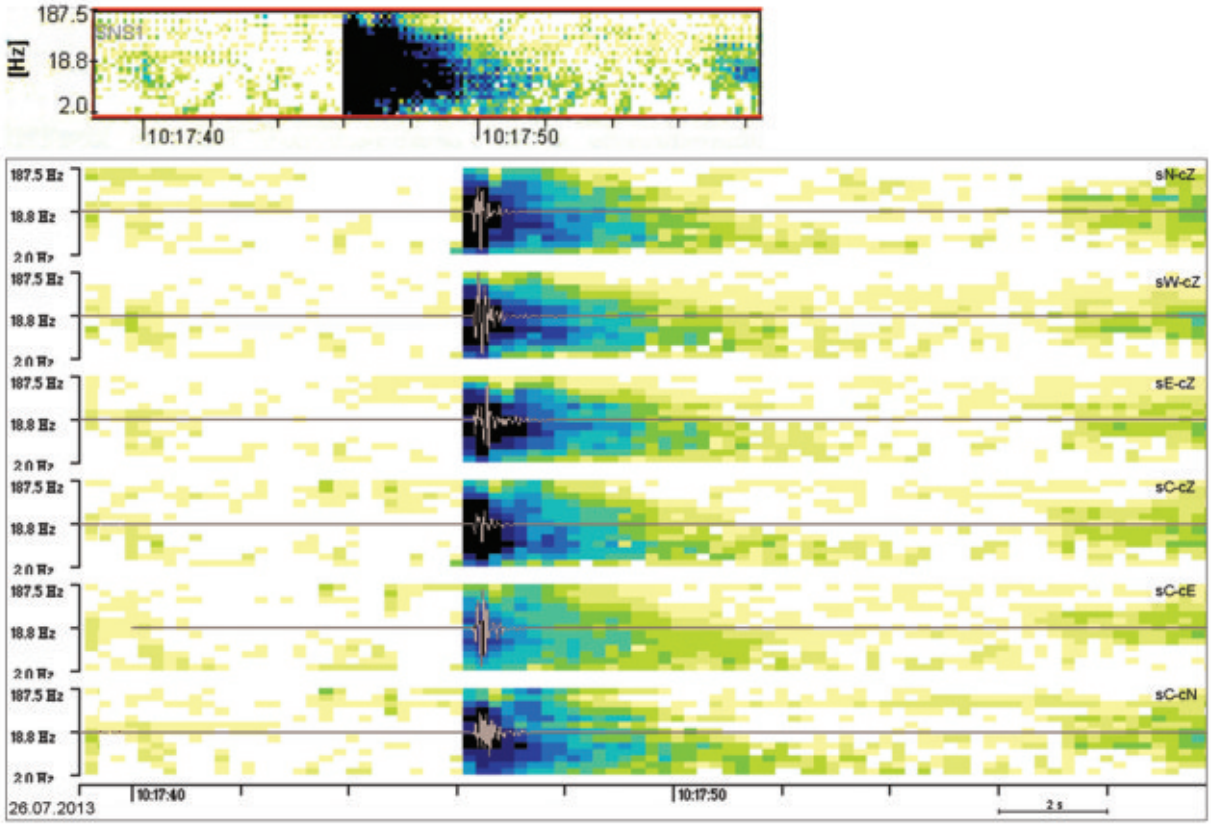

Fig. 6 - Records of the blast occurred in the reference quarry on 26 July 2013 at 10:17:46 UTC. Supersonogram (up) and sonograms with overlaid seismograms (down) for the four stations: vertical component for stations N, W and E, vertical component and horizontal components for station C

EVENT DETECTION AND CHARACTERISATION

BLASTS

Blasts (Fig. 6), with a duration varying from 3 to 7 seconds, enlighten a wide range of frequencies (2-187 Hz) upon arrival of P-waves and show a tail focused by frequencies in a range between 2 and 50 Hz.

By analysing the three events of known location that occurred in the reference quarry, a subsoil model was fixed in order to define the hypocentral coordinates of events of unknown location, i.e. both other blasts in the quarry district and rock failure events. In particular, by changing the subsoil properties in the software tool, the best fit between modelled and recorded locations was obtained with a homogeneous half-space model having a P-wave velocity of 2.7 km/s and a V_P/V_S ratio of 1.73. The so resulting subsoil model is consistent with a rock mass of good quality confirmed by the geomechanical surveys. Considering all of the recorded 15 blasts, the M_L ranges from -0.1 to 0.8.

The physical analysis of the blasts with the SAC software showed that the PGA, PGV and AI values calculated on the horizontal components were always higher than those calculated on the vertical component. Considering the values of the horizontal components for the 15 blasts, PGA_h ranged between 10^{-2} m/s^2 and 10^{-3} m/s^2, PGV_h between 10^{-4} m/s and 10^{-6} m/s, while AI_h was of 10^{-6} m/s to 10^{-11} m/s.

NANOSEISMIC EVENTS CORRESPONDING TO GRAVITY-INDUCED SLOPE INSTABILITIES

The analysis of the collected seismic data with the SonoView tool revealed 27 events that might be associated with gravity-induced slope instabilities. All these events, including 23 collapses and 4 failures related to rock mass fracturing, were recorded during the survey of 26-27 July 2013 and were distinguished on the basis of waveform features (Fig. 7). Collapses are typically characterised by short duration (less than 1 s) and frequency content from 5 to 50 Hz. Conversely, failures are characterised by longer duration (3-6 s) and frequency content of 2-50 Hz upon the first arrival of P-waves, while the frequency content of the signal tail is limited to a closer range, i.e. 2-10 Hz.

By analysing the events with HypoLine, the M_L ranged from -1.3 to -2.3 for collapses and from -1.0 to -1.4 for failures. While

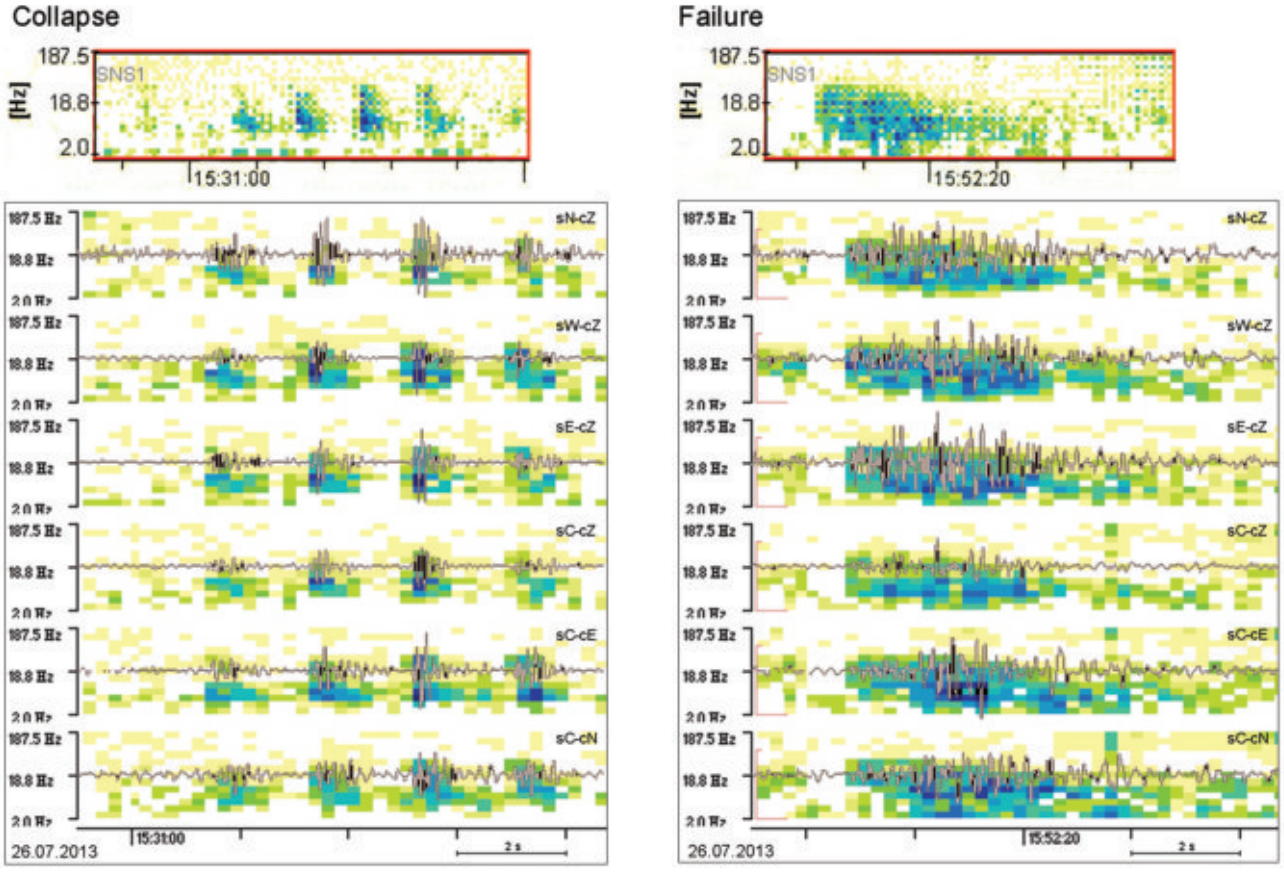

Fig. 7 - Events recorded on 26 July 2013: four collapses beginning at 15:31:01 UTC and failures at 15:52:16 UTC. Supersonogram (up) and sonograms with overlaid seismograms (down) for the four stations: vertical component for stations N, W and E, vertical component and horizontal components for station C

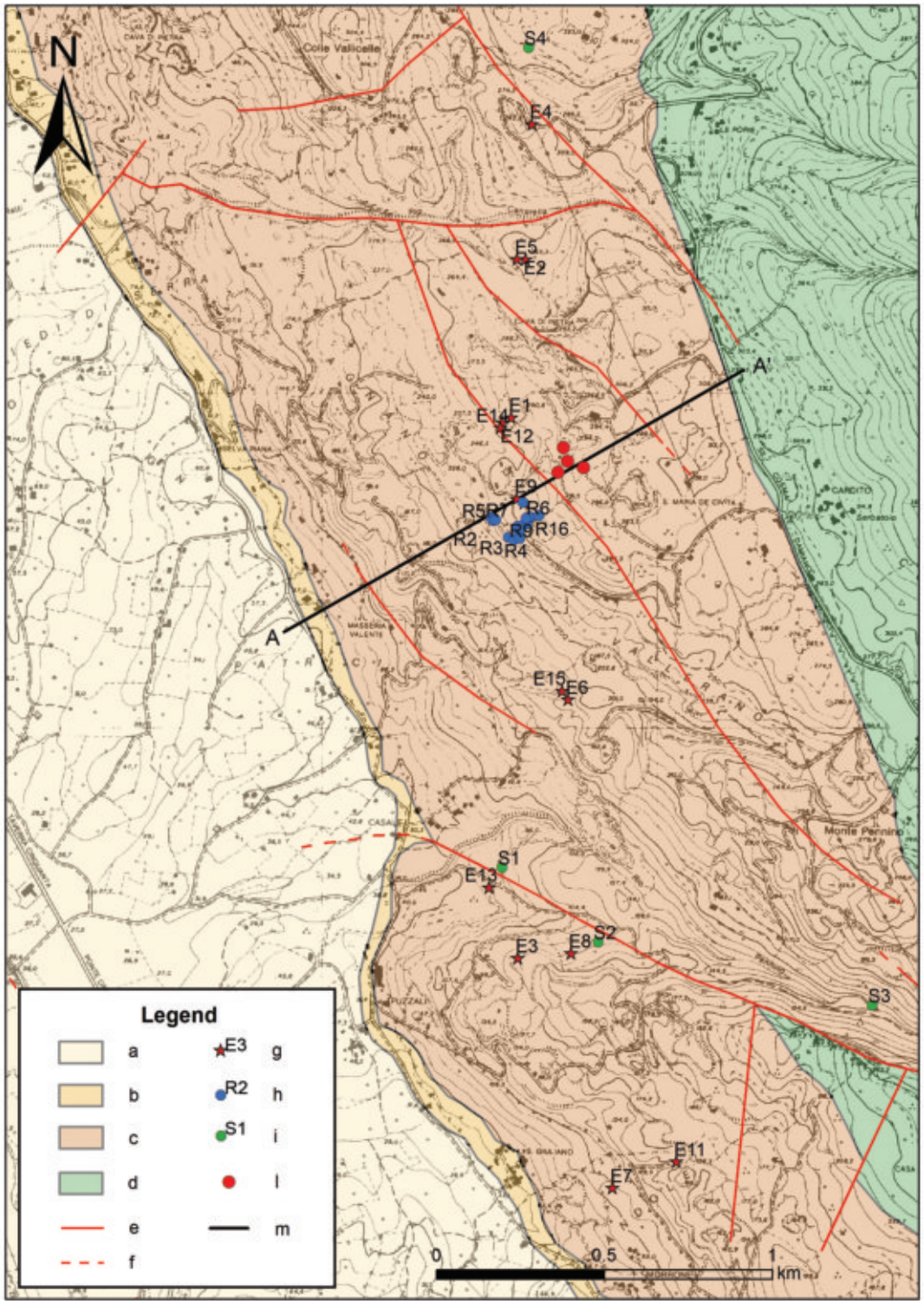

Fig. 8 - Geological map with epicentre of the identified event. LEGEND: a) Flysch argilloso-arenaceo (Tortonian-Messinian); b) Marne ad orbulina (Serravallian-Tortonian); c) Calcari a briozoi e litotamni (Langhian-Serrravallian); d) Calcari bianchi e avana (Cenomanian-Danian); e) fault; f) supposed fault; g) blast (with event ID); h) collapse (with event ID); i) failure (with event ID); l) SNS array station; m) trace of the geological cross-section (see Fig. 9)

the 4 failures were located in different sectors of the quarry district, collapses had a fairly small source area, S-W of the SNS array (Figs. 8 and 9), at a distance of roughly 300 m and with a scatter of about 60 m. This source area did not correspond to the reference wall.

The physical analysis of collapses showed that the PGA, PGV and AI values for horizontal components were higher than those for vertical ones; on the other hand, as it regards failures, the same parameters had quite similar values for the different components. For collapses, the following ranges were obtained: PGA_h of 10^{-4} to 10^{-5} m/s^2, PGV_h of 10^{-6} to 10^{-7} m/s and AI_h of 10^{-10} to 10^{-11} m/s. For failures, PGA_h was in the range of 10^{-5} m/s^2, PGV_h was of 10^{-6} to 10^{-7} m/s and AI_h of 10^{-10} to 10^{-11} m/s.

Table 2 summarises the main physical properties of the three types of events (blasts, collapses and failures) detected and characterised during the three measurement campaigns in the quarry district of Coreno Ausonio.

DISCUSSION

To better constrain the detection analysis performed through the NanoseismicSuite software, changes of the seismic ambient noise were analysed throughout the period of the 26-27 July 2013 measurement campaign, during which the events related to gravity-induced slope instability were identified. This analysis aimed at excluding that the events detected as collapses and failures might be directly related to the use of mechanical equipment. By the Geopsy software (www.geopsy.org), each daily trace was split into 1-h intervals and, for each interval, the Fast Fourier Transform (FFT) was calculated on 40-s windows. Based on the resulting 24 mean amplitude spectra, the change of the maximum spectral amplitude over the 24 hours was analysed for four frequency intervals considered as significant: 1-2 Hz, 4-5 Hz, 8-10 Hz and 15-20 Hz (Fig. 10).

Among the four frequency ranges considered, the 1-2 Hz range was the only one that stood around significant levels

Type of event	Events (n)	Duration (s)	Typical frequencies (Hz)	M_L	PGA_h (m/s^2)	PGV_h (m/s)	AI_h (m/s)
Blast	15	3-7	2-187 tail 2-50	0.8/-0.1	$10^{-2}/10^{-3}$	$10^{-4}/10^{-6}$	$10^{-6}/10^{-11}$
Collapse	23	<1	5-50	-1.3/-2.3	$10^{-4}/10^{-5}$	$10^{-6}/10^{-7}$	$10^{-10}/10^{-11}$
Failure	4	3-6	2-50 tail 2-10	-1.0/-1.4	10^{-5}	$10^{-6}/10^{-7}$	$10^{-10}/10^{-11}$

Tab. 2 - Main physical properties of the events recorded and detected during the 3 measurement campaigns

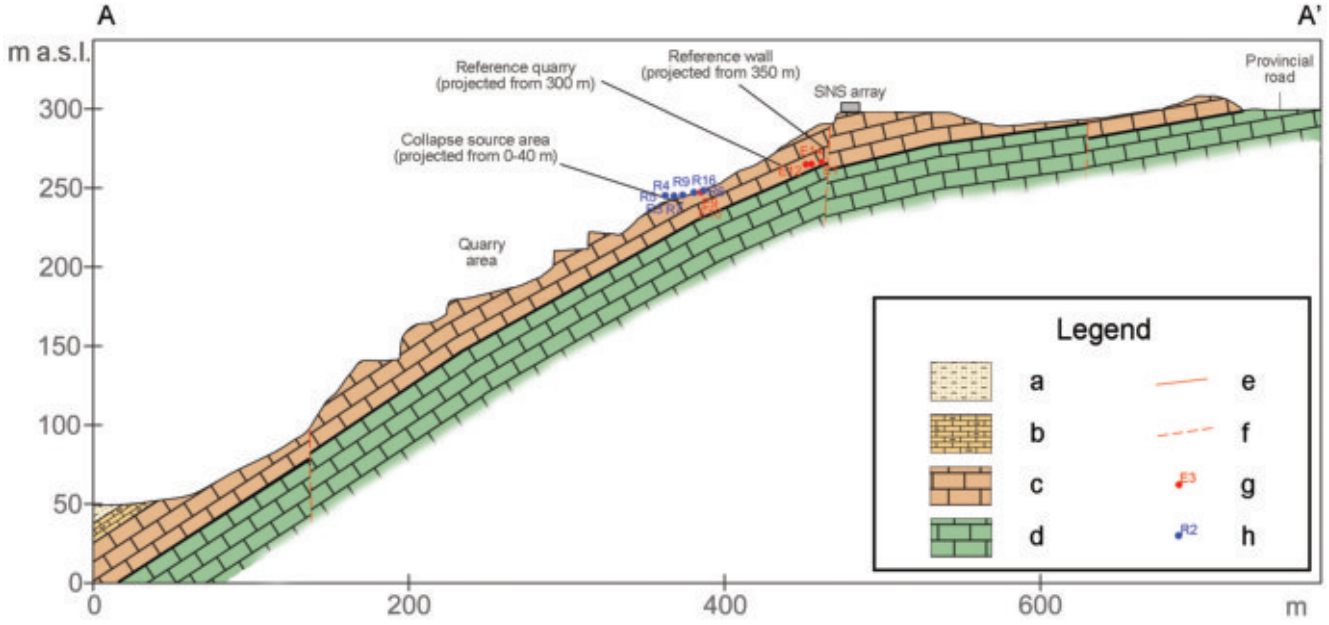

Fig. 9 - Geological cross-section (trace AA', see Fig. 8) with hypocentre of the identified events. LEGEND: a) Flysch argilloso-arenaceo (Tortonian-Messinian); b) Marne ad orbulina (Serravallian-Tortonian); c) Calcari a briozoi e litotamni (Langhian-Serrravallian); d) Calcari bianchi e avana (Cenomanian-Danian); e) fault; f) supposed fault; g) blast (with event ID); h) collapse (with event ID)

over the 24 hours and was therefore associated with the typical frequency of the site; this range was clearly discernible at night, when the other frequencies were not powered. All other frequency ranges yielded a significant FFT amplitude only in quarry working hours (indicatively from 4:30 UTC to 14:00 UTC). As a consequence, the FFT amplitude of these frequencies may be associated with the use of the equipment needed to quarry and work the rocky material. In particular, the 15-20 Hz interval well corresponds to the events pointed out by the supersonogram: most of the events were detected from 15:00 UTC on, in a period where the noise spectral amplitude was lower than the one in quarry working hours (dropping to about 1/10 for horizontal components and to about 1/4 for the vertical component). This result infers that the quarrying equipment was not in operation and thus that the identified slope instability events were related to the settlement of the rock mass.

The source area of the detected collapses (Fig. 11) corresponds to an abandoned quarry, on which a service-road was realised. The road rests on man-made fill, composed of limestone clasts having heterogeneous sizes (from centimetre-scale clasts up to 1 m-size blocks). Loose heterogeneous-size debris lies at the foot of the abandoned quarry wall and along the roadsides. The abandoned quarry wall has a different orientation if compared to the reference wall but the surveyed joint sets have the same attitude. Slope stability analyses performed for this wall by the Wedge Failure Analysis software output a suitability for wedge sliding related to two of the existing joint sets; the corresponding SF value is of 2.3, i.e. lower than those obtained for the reference wall. On the contrary, as it regards planar sliding and toppling, the attitude of the joint sets in correspondence to the rock wall fails to satisfy the kinematic conditions suitable for the failure mechanisms.

In conclusion, two possible sources were identified for the recorded seismic events : i) falls of the limestone blocks from the man-made fill; ii) rock slides along joints isolating the rock

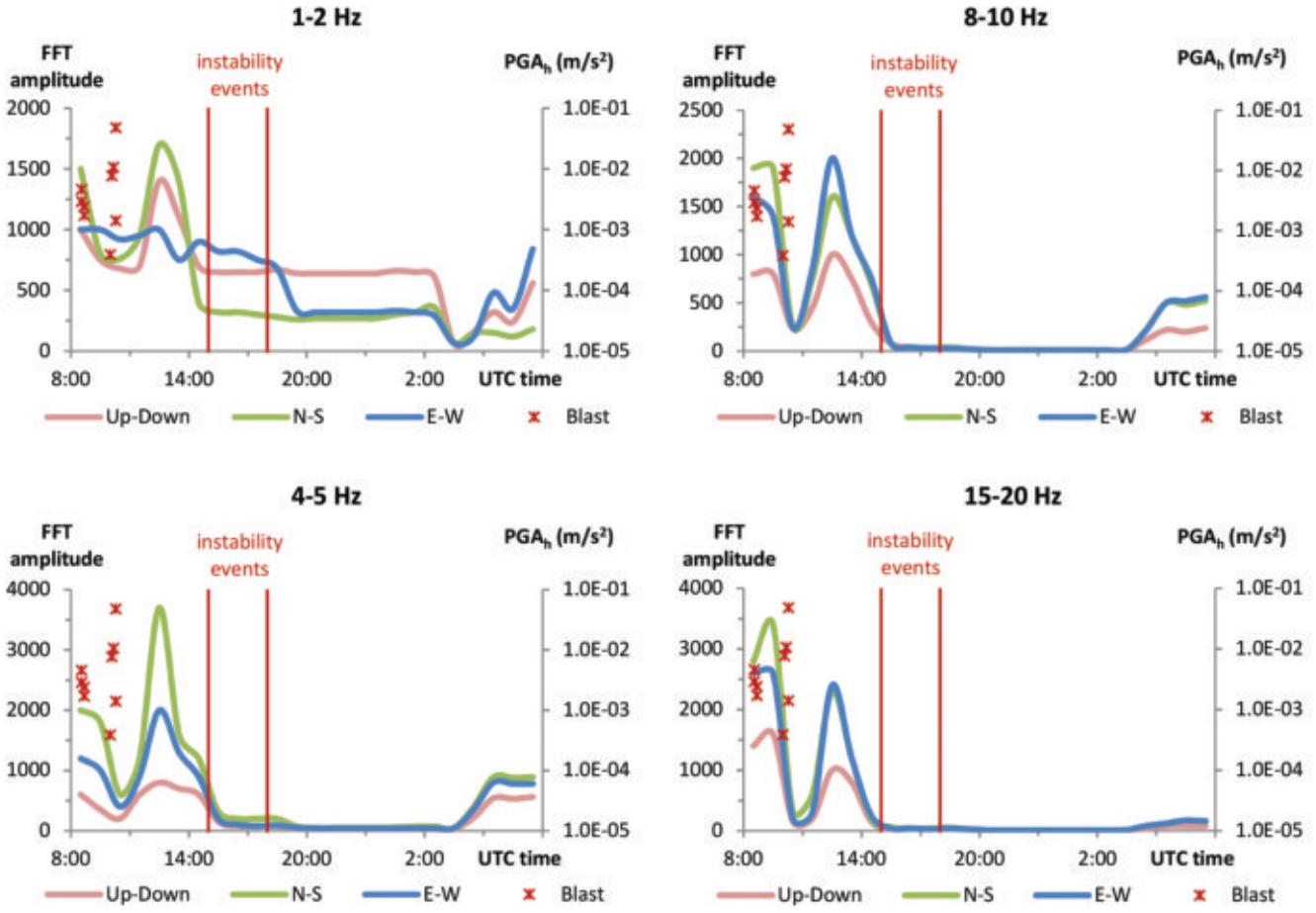

Fig. 10 - Variation measured in the maximum FFT amplitude (referred to the left y axis) for four selected frequency intervals (1-2 Hz, 4-5 Hz, 8-10 Hz e 15-20 Hz) in the time period: 08:00 UTC of 26 July 2013 - 08:00 UTC of 27 July 2013; the red crosses indicate the PGA$_h$ values of the blasts (referred to the right y axis); the two vertical red lines track the time period in which the highest number of gravity-induced slope instability events was recorded

wedges on rock walls.

As it regards the time of occurrence of the slope instability events detected in the 26-27 July 2013 measurement campaign (Fig. 12), they were mostly recorded during hours following the end of work in the quarry district, i.e. when the ambient seismic noise was significantly lower. On the contrary, the supersonogram of the records obtained during the working hours was hardly analysable due to the equipment used for working limestone blocks. As this equipment represented an intermittent vibrational source, its effect in terms of amplitude spectral content was not negligible and could not be removed so affecting many tracks of the supersonogram signal. This condition did not avoid to detect high-energy events (e.g. blasts), i.e. by distinguishing them from the noise, while, on the contrary, in case of low-energy events (e.g. additional gravity-induced slope instability events) their occurrence could be nor excluded neither confirmed. This is because such events may have taken place during quarry working hours, but their signals in the supersonogram may have been masked by the other active sources of vibration in the quarry district.

The horizontal PGA value of the events recorded during the 26-27 July measurement campaign gradually decreased in the hours following the blasts, in spite of the potential gap of events in quarry working hours; indeed, the highest acceleration values were recorded in the first events detected after the end of quarry working hours.

The highest number of blasts (9) and their highest intensity was observed during the 26-27 July 2013 measurement campaign and the higher solicitation of the system might justify the higher number of the effects.

CONCLUSIONS

During 2013, an experiment was performed in the quarry district of Coreno Ausonio (central Italy) to test the nanoseismic monitoring technique for detecting effects of slope instabilities induced by fast changes in stress conditions of rock masses outcropping on quarry walls, due to the quarrying activities and, in particular, to blasting.

Nanoseismic signals, recorded during three measurement campaigns, made it possible to detect 15 blasts followed by 27 vibrational events related to gravity-induced slope instabilities. Based on duration and frequency content, 23 collapses and 4 failures were distinguished among the recorded slope instability events. By using the NanoseismicSuite software, a subsoil

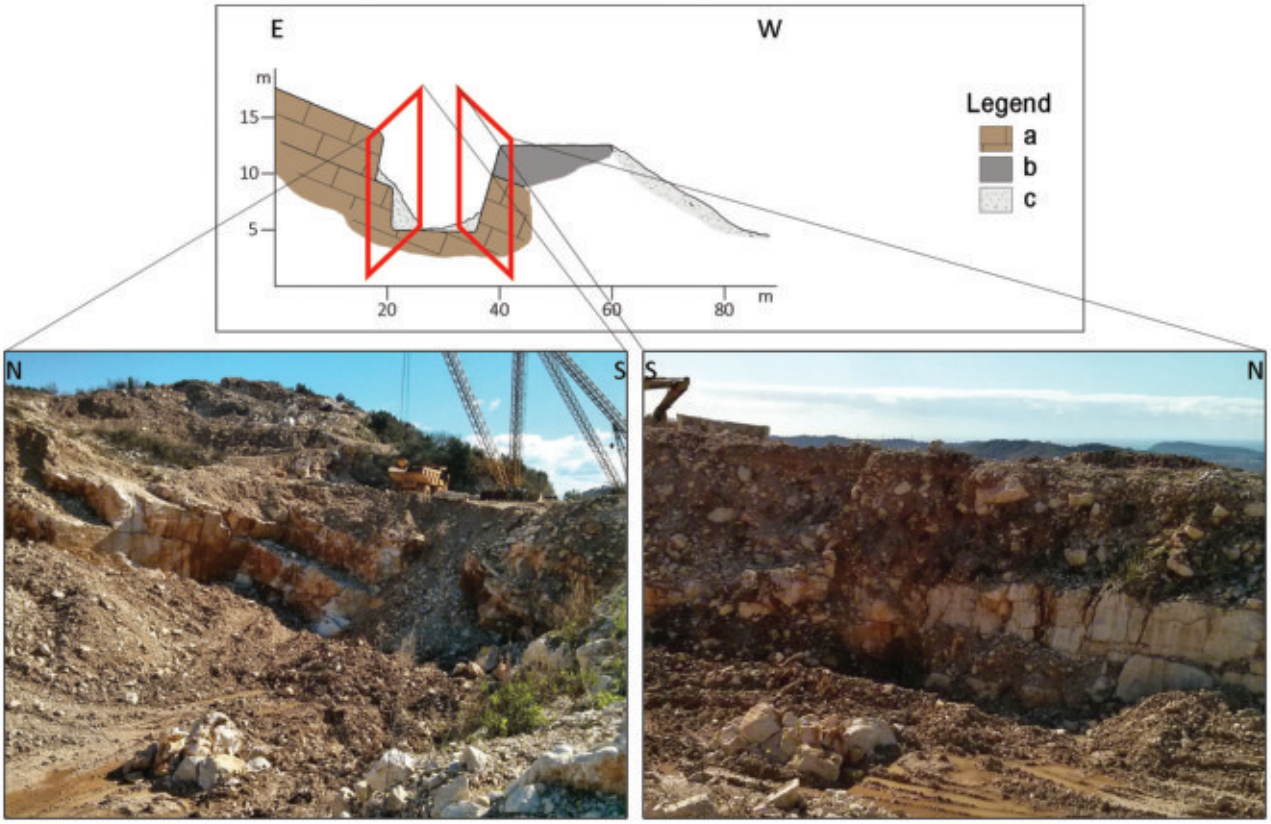

Fig. 11 - Schematic section and photos of the identified collapses source area. LEGEND: a) jointed rock mass; b) man-made fill; c) debris with heterogeneous-size clasts

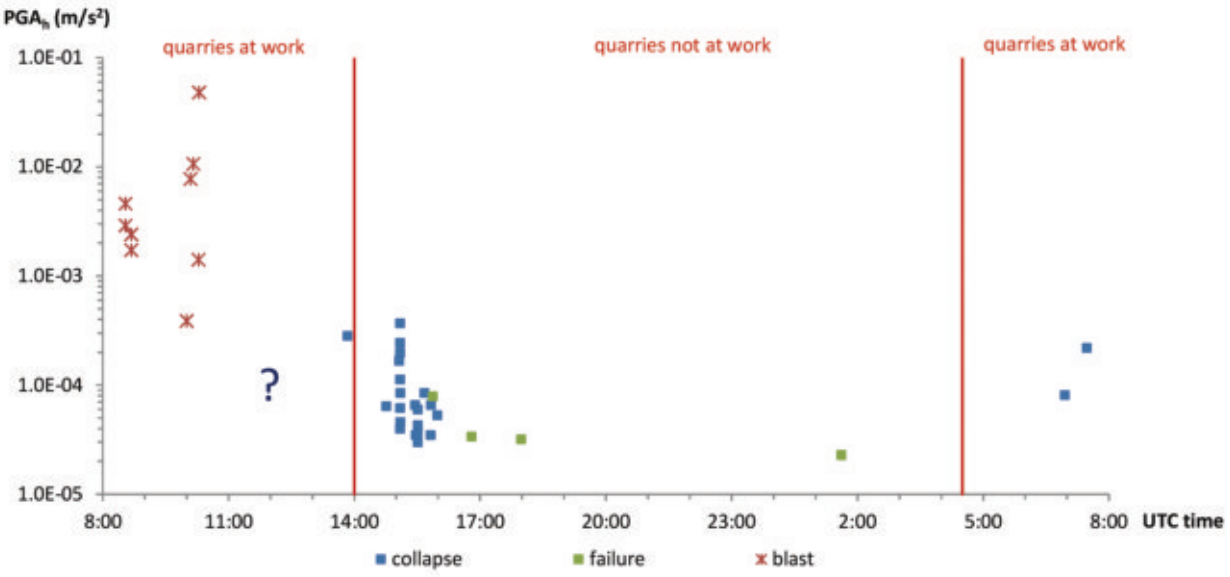

Fig. 12 - Time vs. PGA$_h$ for the events recorded in the 26-27 July 2013 measurement campaigns; the question point indicates a period in which occurrence of gravity-induced slope instability events could be nor excluded neither confirmed because of their signals in the supersonogram may have been masked by vibration related to the quarry working equipment

model was fixed based on 3 blasts of well-known location from a reference quarry. This model (homogeneous half-space with V_P of 2.7 km/s and V_P/V_S ratio of 1.73) was used to define the hypocentre and the M_L also in case of events with unknown location. By defining the hypocentre of the detected collapses, an area more prone to gravity-induced instability was identified. As the events were recorded only in the 26-27 July measurement campaign and over a time period fairly close to the blasts, such an evidence may be related to the higher stresses caused by quarrying in this survey (9 blasts much more energetic than the 3 blasts recorded in the two other surveys).

In conclusion, the experimental test of nanoseismic monitoring performed in the Coreno Ausonio quarrying-by-blasting site yielded appreciable results. The experiment also highlighted some limitations of the nanoseismometric technique when it is associated with intense man-induced noise, i.e. generated in the quarry site during working hours. Nonetheless, the technique proved to be a useful tool to track small-scale rock landslides (e.g. detachment of blocks, sliding of debris) induced by man-made blasting.

ACKNOWLEDGEMENTS

The Authors are thankful to Achille Germanelli, Walter Salvatore and to the entire "Consorzio per la Valorizzazione del Perlato Coreno" for providing support during the experimental stage and for making their spaces available for the installation of the nanoseismic array. The Authors also thank the Institute of Geophysics of the Stuttgart University for the use of the NanoseismicSuite software as well as Stefano Rivellino and Luca Lenti for their suggestions in the data processing.

REFERENCES

Accordi B., Angelucci A. & Sirna G. (1969) - *Note illustrative della carta geologica d'Italia alla scala 1:100.000. Foglio 159: Frosinone. Foglio 160: Cassino.* Servizio Geologico d'Italia, Roma (IT).

Accordi G., Carbone F., Civitelli G., Corda L., De Rita D., Esu D., Funiciello R., Kotsakis T., Mariotti G. & Sposato A. (1986) - *Lithofacies map of Latium-Abruzzi and neighbouring areas.* Quaderni C.N.R. La Ricerca Scientifica, **114** (5): 223.

Amitrano D., Arattano M., Chiarle M., Mortara G., Occchiena C., Pirulli M. & Scavia C. (2010) - *Microseismic activity analysis for the study of the rupture mechanism in unstable rock masses.* Nat. Hazard Earth Syst. Sci., **10**: 831-841.

ASTM (2008) - *D 5731-08. Standard test method for determination of the Point Load Strength Index of rock and application to rock strength classifications.* In: ASTM Volume 04.08 Soil and Rock (I). Author, Philadelphia (PA).

Bally A.W., Burbi L., Cooper C. & Ghelardoni R. (1988) - *Balanced sections and seismic reflection profiles across the central Apennines*. Mem. Soc. Geol. It., **35**: 257-310.

Barton N. & Choubey V. (1977) - *The shear strength of rock joints in theory and practice.* Rock Mech., **10** (1-2): 1-54.

Brunamonte F., Prestininzi A. & Romagnoli C. (1996) - *Geomorfologia e caratteri geotecnici dei depositi di terre rosse nelle aree carsiche degli Aurunci Orientali (Lazio meridionale, Italia)*. Geologica Romana, **30**: 465-478.

Deparis J., Jongmans J., Cotton F., Bailler L., Thouvenot F. & Hantz D. (2008) - *Analysis of rock-fall and rock-fall avalanche seismograms in the French Alps.* Bull. Seism. Soc. Am., **98** (2): 1781-1796.

Cipollari P. & Cosentino D. (1992) - *Considerazioni sulla strutturazione della catena dei Monti Aurunci: vincoli stratigrafici.* Studi Geologici Camerti, Vol. Spec. 1991/2: 151-156.

Cipollari P. & Cosentino D. (1997) - *Il sistema Tirreno-Appennino: segmentazione litosferica e propagazione del fronte compressivo.* Studi Geologici Camerti, Vol. Spec. 1995/2: 125-134.

Evans S., Scarascia Mugnozza G. & Strom A. (2006) - *Landslides from massive rock slope failure.* Nato Science Series, Springer, Netherlands. Series IV: Earth Environ. Sci., **49**: 662.

Fiorucci M., Iannucci R., Lenti L., Martino S., Paciello A., Prestininzi A. & Rivellino S. (2016) - *Nanoseismic monitoring of gravity-induced slope instabilities for the risk management of an aqueduct infrastructure in Central Apennines (Italy).* Nat. Hazards. DOI: 10.1007/s11069-016-2516-5

Got J.-L., Mourot P. & Grangeon J. (2010) - *Pre-failure behaviour of an unstable limestone cliff from displacement and seismic data.* Nat. Hazard. Earth Syst. Sci., **10**: 819-829.

ISRM (1978) - *Suggested methods for the quantitative description of discontinuities in rock masses.* Int. J. Rock Mech. Min. Sci. & Geomech. Abstr., **15**: 319-368.

Hoek E. & Bray J.W. (1981) - *Rock slope engineering.* Institution of Mining and Metallurgy, London (UK).

Hudyma M. & Potvin Y.H. (2010) - *An engineering approach to seismic risk management in hardrock mines*. Rock Mech. Rock Eng., **43**: 891-906.

Joswig M. (1990) - *Pattern recognition for earthquake detection.* Bull. Seism. Soc. Am., **80** (1): 170-186.

Joswig M. (1995) - *Automated classification of local earthquake data in the BUG small array*. Geophys. J. Int., **120**: 262-286.

Joswig M. (2008) - *Nanoseismic monitoring fills the gap between microseismic networks and passive seismic*. First Break, **26**: 121-128.

Lenti L., Martino S., Paciello A., Prestininzi A. & Rivellino S. (2012) - *Microseismicity within a karstified rock mass due to cracks and collapses triggered by earthquakes and gravitational deformations.* Nat. Hazards, **64**: 359-379.

Markland J.T. (1972) - *A useful technique for estimating the stability of rock slopes when the rigid wedge slide type of failure is expected.* Imperial College Rock Mechanics Research Reprints, **19**.

Phillips W.S., Pearson D.C., Edwards C.L. & Stump B.W. (1997) - *Microseismicity induced by a controlled, mine collapse at white pine, Michigan*. Int. J. Rock Mech. Min. Sci., **34**: 314, paper 246.

Putignano M.L. & Ungaro A. (1996) - *Considerazioni sulla provenienza delle intercalazioni carbonatiche nella successione terrigena messiniana nella Valle dell'Ausente.* Mem. Soc. Geo. It., **51** (1): 351-362.

Sick B., Walter M. & Joswig M. (2014) - *Visual event screening of continuous seismic data by supersonograms.* Pure Appl. Geophys., **171**: 549-559. DOI: 10.1007/s00024-012-0618-x

Szwedzicki T. (2003) - *Rock mass behaviour prior to failure.* Int. J. Rock Mech. Min. Sci., **40**: 573-584.

Tang C., Li L., Xu N. & Ma K. (2015) - *Microseismic monitoring and numerical simulation on the stability of high-steep rock slopes in hydropower engineering.* Journal of Rock Mechanics and Geotechnical Engineering, **7**: 493-508.

Walter M., Schwaderer U. & Joswig M. (2012a) - *Seismic monitoring of precursory fracture signals from a destructive rockfall in the Vorarlberg Alps, Austria.* Nat. Hazards Earth Syst. Sci., **12**: 3545-3555.

Walter M., Arnhardt C. & Joswig M. (2012b) - *Seismic monitoring of rockfalls, slide quakes and fissure development at the Super-Sauze mudslide, French Alps.* Eng. Geol., **128**: 12-22.

Wust-Bloch G.H. & Joswig M. (2006) - *Pre-collapse identification of sinkholes in unconsolidated media at Dead Sea area by 'nanoseismic monitoring' (graphical jackknife location of weak sources by few, low-SNR records)*. Geophys. J. Int., **167**: 1220-1232.

Received May 2016 - Accepted September 2016